Dehydrogenation of Ethane to Ethylene via Radical Pathways Enhanced by Alkali Metal Based Catalyst in Oxysteam Condition

Kazuhiro Takanabe and Salman Shahid
King Abdullah University of Science and Technology (KAUST), KAUST Catalysis Center (KCC), Physical Sciences and Engineering Division (PSE), 4700 KAUST, Thuwal 23955-6900, Saudi Arabia

DOI 10.1002/aic.15447
Published online August 21, 2016 in Wiley Online Library (wileyonlinelibrary.com)

The dehydrogenation of ethane to ethylene in the presence of oxygen and water was conducted using Na_2WO_4/SiO_2 catalyst at high temperatures. At 923 K, the conversion rate without water was proportional to ethane pressure and a half order of oxygen pressure, consistent with a kinetically relevant step where an ethane molecule is activated with dissociated oxygen on the surface. When water was present, the ethane conversion rate was drastically enhanced. An additional term in the rate expression was proportional to a quarter of the oxygen pressure and a half order of the water pressure. This mechanism is consistent with the quasi-equilibrated OH radical formation with subsequent ethane activation. The attainable yield can be accurately described by taking the water contribution into consideration. At high conversion levels at 1073 K, the C_2H_4 yield exceeded 60% in a single-pass conversion. The C_2H_4 selectivity was almost insensitive to the C_2H_6 and O_2 pressures. © 2016 The Authors AIChE Journal published by Wiley Periodicals, Inc. on behalf of American Institute of Chemical Engineers *AIChE J*, 63: 105–110, 2017
Keywords: catalysis, reaction kinetics, hydrocarbon processing

Introduction

The oxidative dehydrogenation (ODH) of ethane to ethylene has some advantages over the non-oxidative counterpart because of the higher expected rates and fewer thermodynamic constraints.[1] Detailed information of this catalytic reaction can be found in excellent review articles in the literature.[2–6] The attainable yields are largely associated with the reactivity of oxygen species, which activates the C–H bonds of ethane and ethylene at different rates. The ethylene selectivity decreases with increasing ethane conversion because of the competitive ethylene oxidation to CO_x as a secondary reaction when the ethylene concentration increases. There are basically two types of catalysts: redox catalysts (mainly V- or Mo-based catalysts) and alkali-metal (halide) catalysts.[6] In particular, when an alkali-metal catalyst is used (mainly Li-based catalysts),[7] it is proposed that a complex reaction mechanism is involved, where the catalytic surface participates in radical formations in homogeneous gas phase reactions.

A similar heterogeneous (surface)-homogeneous (gas-phase) reaction pathway has been discussed during the oxidative coupling of methane (OCM).[8–14] Our previous works on alkali-metal-based catalysts show the beneficial effects of water to improve the OCM rate and C_2 selectivity.[15–17] This water effect is exceptionally unique for Na_2WO_4/SiO_2 catalysts, with which notably high OCM attainable yields have been reported (C_{2+} yields >25%).[17] In the absence of water, the rates were proportional to $P_{CH_4}P_{O_2}^{0.5}$.[17] When H_2O is present, the methane conversion rates were proportional to $P_{O_2}^{0.25}P_{H_2O}^{0.5}$, consistent with the quasi-equilibrated OH radical formation from the O_2–H_2O mixture, which in turn subtracts hydrogen from CH_4.[17] Identical kinetics was obtained in both a recirculating-batch reactor and a fixed-bed reactor,[14–17] which validates the obtained rate expressions. The selective OCM catalyst in this series of catalysts is required to paradoxically catalyze H_2O instead of CH_4 on the surface.

Kinetic analyses on the Na_2WO_4/SiO_2, Na_2WO_4/Al_2O_3, K_2WO_4/SiO_2, Na_2MoO_4/SiO_2, and Na_2CO_3/SiO_2 OCM catalysts suggest that Mn, W, Mo, and SiO_2 are not essential to give water activation but alkali metals are.[17] This result suggests that the redox properties of specific oxides (such as Mn) do not play an important role, but alkali metal peroxide-like intermediates are expected to be involved. For example, the presence of Mn in the catalyst component improves the OCM rate because it mildly combusts CH_4 to generate H_2O, which subsequently selectively catalyzes to produce C_2.[17] Such metals are not required if the water is co-fed to make an oxysteam condition. It should be noted that many alkali-metal-based salts such as Na_2WO_4 melt on the catalyst surface during high-temperature reactions because the melting point of the alkali salt is lower than the OCM reaction temperature. This melting makes the support material sinter (e.g., cristobalite formation in the case of SiO_2),[17,18] which reduces the surface area of the catalyst, prevents the bare support and/or impurity surface from exposure, and suppresses the combustion that is prevalent for the high-temperature reaction.[17]

Correspondence concerning this article should be addressed to K. Takanabe at kazuhiro.takanabe@kaust.edu.sa.

This study is an extension of the unique water effects that were found during the OCM to apply to the ODH of ethane. Therefore, the reaction is expected to proceed in radical homogeneous pathways. In this study, we intend to introduce the similar kinetic contribution of water in homogeneous gas phase reactions that are induced by the Na_2WO_4/SiO_2 catalyst. The enhancement in rate by water was observed, which is consistent with the additional water term in the rate expression to convert hydrocarbons. This rate expression will provide new insight into the ODH reaction mechanism and an accurate description of the attainable ODH yield.

Experimental

For the catalyst preparation, SiO_2 (Sigma-Aldrich, Silica Gel, Davisil Grade 646, 35–60 mesh) was used as a support to immobilize 10 wt % Na using $Na_2WO_4{\cdot}2H_2O$ (Sigma-Aldrich, 99%) via wet impregnation. This sample was heated under a dry air flow at 1173 K for 8 h at a rate of 2 K min^{-1}.

The rates and selectivities of the CH_4–O_2–H_2O reactions were measured in flow reactors using a U-shaped quartz cell (4-mm I.D.). The samples (0.8 g) were held onto quartz wool without dilution and almost completely filled in the heated zone. The temperature was maintained using a Honeywell controller, which was coupled to a resistively heated furnace, and measured with a K-type thermocouple set outside the catalyst bed. C_2H_6 (99.995%), 20% O_2 in He, and He (99.999%) were purchased from Abdullah Hashim Industrial Gases & Equipment (AHG) and used after further purifying via filtration. The flow was regulated by mass flow controllers. A saturator with a well-controlled temperature (278–293 K) was used to introduce the H_2O gas.

The reactant and product concentrations were measured using a VARIAN gas chromatograph 450GC with a programmed system. This programmed system involves a molecular sieve 5A column, a HayeSep Q column with a thermal conductivity detector, and a VARIAN CP-Wax 52 CB capillary column with a flame ionization detector. This configuration enables the distinction of all C_1–C_4 hydrocarbons. The conversion, selectivities and yields are reported on a carbon basis as cumulative integral values as follows:

$$X_{C_2H_6}\ (\%) = \frac{(\text{total mols of carbon in products})}{(\text{total mols of } C_2H_6 \text{ in})} \times 100$$

$$\text{or } = \frac{(\text{total mols of carbon in products})}{(\text{total mols of carbon out incl. } C_2H_6)} \times 100$$

$$S_{C_2H_4}\ (\%) = \frac{(\text{mols of carbon in the specific product})}{(\text{total mols of carbon in products})} \times 100$$

$$Y_{C_2H_4}\ (\%) = X_{C_2H_6}(\%) \times S_{C_2H_4}(\%)/100$$

For rigorous kinetic analyses, linear regression was used to extrapolate the rates that were measured at various conversions to the rates at zero conversion. The obtained rates at zero conversion strictly reflect the input conditions with the given reactant pressures, which minimizes the contribution of the generated heat by the reaction at low conversion levels. The carbon balance was always close to unity during our measurement, suggesting that no carbon deposition or no formation of condensable products was observed.

The N_2 sorption studies were conducted using a Micromeritics ASAP 2420 to determine the Brunauer–Emmett–Teller (BET) surface area. Inductively coupled plasma (ICP) measurements were performed using an Agilent 720 Series ICP-OES instrument (Agilent Technologies). The material was digested in an ETHOS 1 microwave digestion system (Milestone Srl).

Results and Discussion

First, the Na_2WO_4/SiO_2 catalyst was treated at 1173 K under flowing air for extended time. This treatment before ODH was found to be critical to achieve high selectivity to C_2H_4 from C_2H_6. The melting point of Na_2WO_4 is 971 K, which is substantially lower than this treatment temperature; the molten salt state was generated, and excess salt was eluted to be ~4 wt % of Na. It is considered that the molten state generated at high temperature will decorate the surface of the non-selective sites and facilitate the crystal transformation of SiO_2 to the cristobalite phase. The catalyst with the resultant low surface area of ~5 $m^2\ g^{-1}$ became stable for at least a week during the continuous kinetic measurements, which are reported below. Consistently, no loss of Na or surface area was measured before and after the kinetic analyses.

The effect of the water pressure on the C_2H_6 conversion rates using the Na_2WO_4/SiO_2 catalyst at 923 K is evident in Figure 1A, where the rates are plotted as a function of residence time. The C_2H_6 conversion rate increased monotonically with the addition of water into the reactant stream. Figure 1B shows the corresponding C_2H_4 selectivity as a function of the C_2H_6 conversion. In all cases, the C_2H_4 selectivity was maintained high, and it was greater than 97% when the C_2H_6 conversion was ~5%. The measured products were CO_2 and CO (<2%), with minor hydrocarbon products of CH_4 (<1.5%), C_3H_8 (<0.05%), and n-C_4H_8 (<0.1%).

Considering this strong effect of the water pressure on the rates, kinetic analyses using the zero-conversion rates (rates extrapolated to zero conversion) were conducted to isolate the rates in the absence and presence of water. The partial pressure dependencies for C_2H_6 and O_2 on the C_2H_6 conversion rates are shown in Figures 2A, B. These figures show that the zero-conversion rates for C_2H_6 conversion in the absence of water were first order in C_2H_6 pressure and half order in O_2 pressure. The mechanism is consistent with the reaction of dissociated oxygen (reaction 1) with the C_2H_6 molecule, which is a kinetically relevant step (reaction 3), and is similar to the reported kinetics for CH_4 activation[15]:

$$2* + O_2 \rightleftharpoons 2O_{(s)} \quad (1)$$

$$* + C_2H_6 \overset{K_{C_2H_6}}{\rightleftharpoons} C_2H_{6(s)} \quad (2)$$

$$C_2H_{6(s)} + O_{(s)} \xrightarrow{k_{O,C_2H_6}} C_2H_5\cdot + OH_{(s)} + * \quad (3)$$

where * and (s) indicate the empty surface site and surface species, respectively. The recombination of hydroxyls to generate H_2O is omitted from the scheme, which occurs after the kinetically relevant step. Next, Figure 1A shows that the presence of water drastically enhances the ODH rate. The incremental rate in the presence of water compared to that without water has a pressure dependency of $P_{O_2}^{1/4}P_{H_2O}^{1/2}$, as shown in Figure 3, which is consistent with the kinetically relevant mechanism of the quasi-equilibrated OH radical formation (reaction 4) and subsequent C–H bond activation of C_2H_6 (reaction 5).

$$O_2 + 2H_2O \rightleftharpoons 4OH\cdot \quad (4)$$

$$C_2H_6 + OH\cdot \xrightarrow{k_{OH,C_2H_6}} C_2H_5\cdot + H_2O \quad (5)$$

Thus, the overall rate can be described as

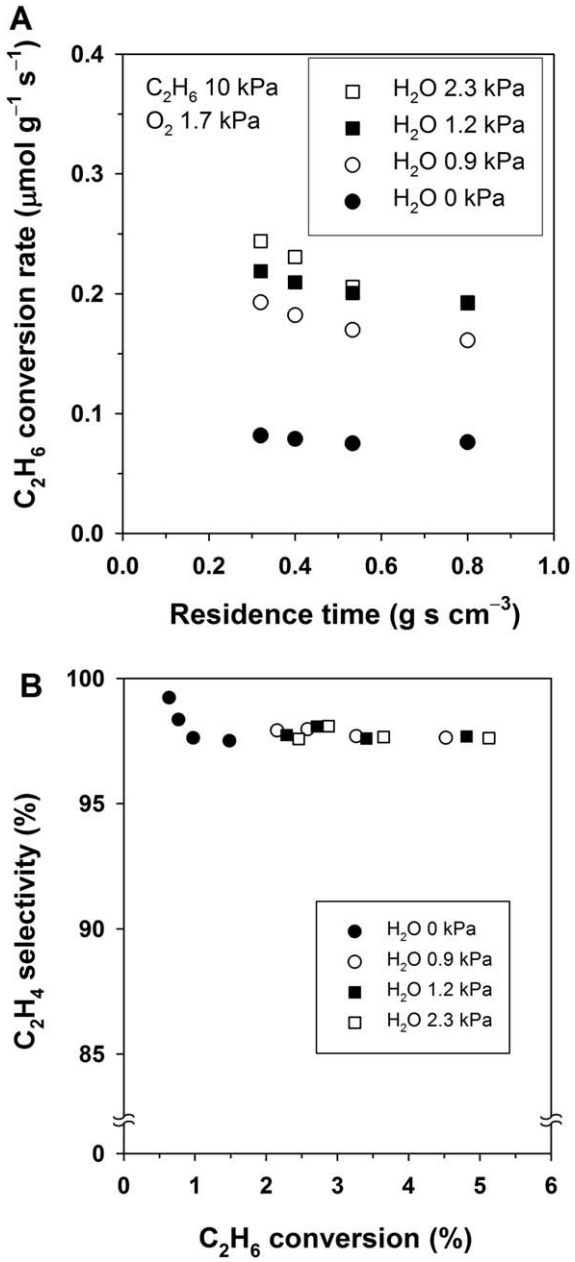

Figure 1. (A) C_2H_6 conversion rate as a function of the residence time at various H_2O pressures and (B) C_2H_4 selectivity as a function of the C_2H_6 conversion at various H_2O pressures and residence time (923 K, Na_2WO_4/SiO_2 0.8 g, C_2H_6 10 kPa, O_2 1.7 kPa, H_2O 0–2.3 kPa).

$$r_{C_2H_6} = r' + r'' = k' P_{C_2H_6} P_{O_2}^{1/2} + k'' P_{C_2H_6} P_{O_2}^{1/4} P_{H_2O}^{1/2} \quad (6)$$

In our previous study, we found that alkali metal is the essential component for the water term in the rate expression.[17] We propose that the Na peroxide species is the critical component during the catalytic cycles, which was originally separately proposed for OCM by Otsuka et al.[19] The difference of this study from the literature is that Na_2O_2 activates H_2O instead of CH_4:

$$2Na_2O_{(s)} + O_2 \rightleftharpoons 2Na_2O_{2(s)} \quad (1')$$

$$H_2O + * \overset{K_{H_2O}}{\rightleftharpoons} H_2O_{(s)} \quad (7)$$

$$Na_2O_{2(s)} + H_2O_{(s)} \rightleftharpoons Na_2O_{(s)} + H_2O_{2(s)or(g)} \quad (8)$$

$$H_2O_{2(s)or(g)} \rightleftharpoons 2OH\cdot \quad (9)$$

In reaction 8, Na_2O_2 activates H_2O to generate the H_2O_2 species either on the surface or in the gas phase, and the generated H_2O_2 decomposes to form OH radicals (reaction 9). The significance of H_2O on the ODH rate suggests that the catalyst can preferentially activate H_2O compared to C_2H_6. It is reasonable to consider that H_2O has a higher adsorption capability than C_2H_6 does. In other words, the rate constants k' and k'' in Eq. 6 have the term of adsorption of the reactant ($K_{C_2H_6}$ and K_{H_2O} in reactions 2 and 7), which may account for this difference. It is reasonable to consider adsorption before the bond activation because the O–H bond in H_2O (497 kJ mol^{-1}) is stronger than the C–H bond in C_2H_6 (423 kJ mol^{-1}) and C_2H_4

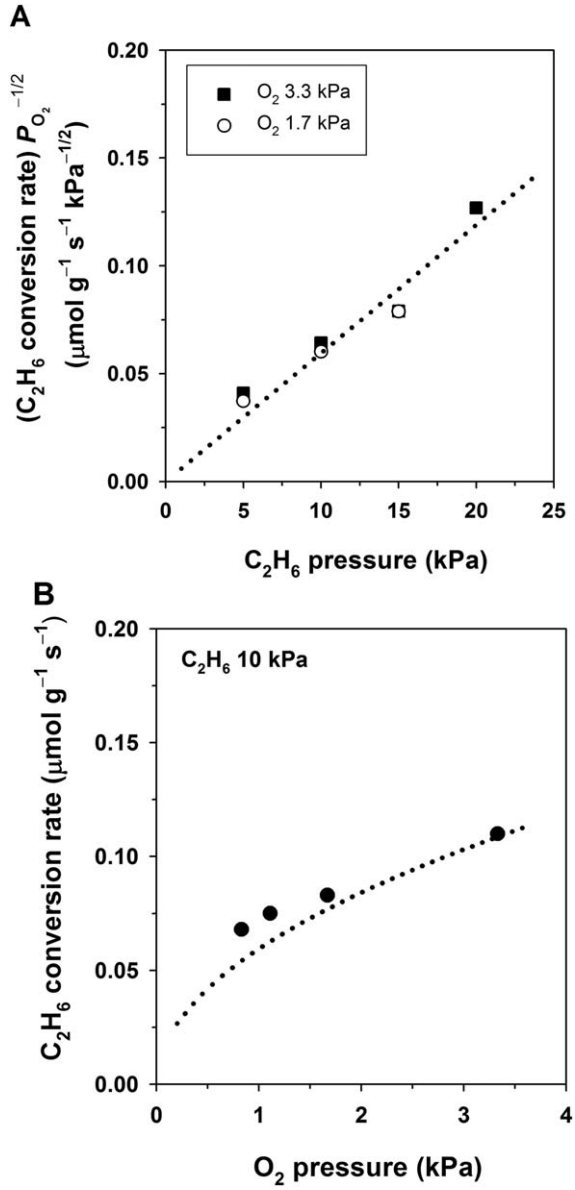

Figure 2. Zero C_2H_6 conversion rate as a function of the (A) C_2H_6 pressure and (B) O_2 pressure (923 K, Na_2WO_4/SiO_2 0.8 g).

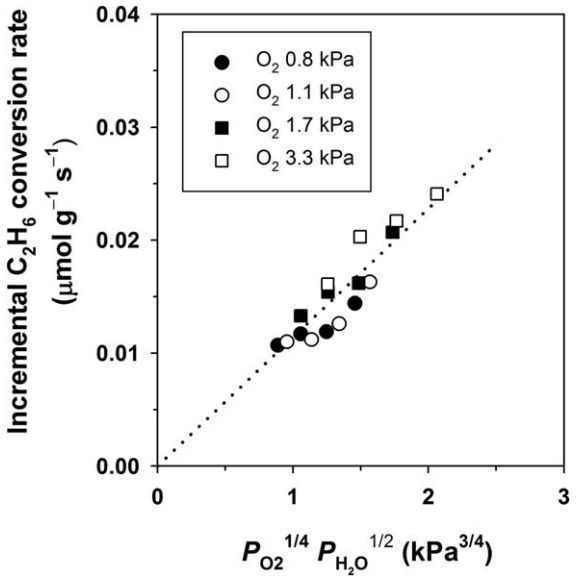

Figure 3. Incremental C_2H_6 conversion rate (r'') as a function of the C_2H_6 pressure (923 K, Na_2WO_4/SiO_2 0.8 g, C_2H_6 5–20 kPa, O_2 0.8–3.3 kPa, H_2O 0.9–2.3 kPa).

(463 kJ mol^{-1}),[20] when the molecules are intact with other molecules or surface.

Figure 4 shows the temperature dependence of k' and k'' in the above equation. The apparent activation energies for these two rate constants, which are $E'_{a,app}$ and $E''_{a,app}$, respectively, are both ~181 kJ mol^{-1}. The formation enthalpies of Na_2O_2 and Na_2O are −515 and −416 kJ mol^{-1}, respectively. Thus, the enthalpy ΔH_O for the quasi-equilibrated step (reaction 1′) is −99 kJ mol^{-1}.

$$E'_{a,app} = E_{a,O*} + \frac{1}{2}\Delta H_O \tag{10}$$

Therefore, the estimated activation energy $E_{a,O*}$ of reaction 3 is 130 kJ mol^{-1}. Some reports describe that Na_2O_2 can

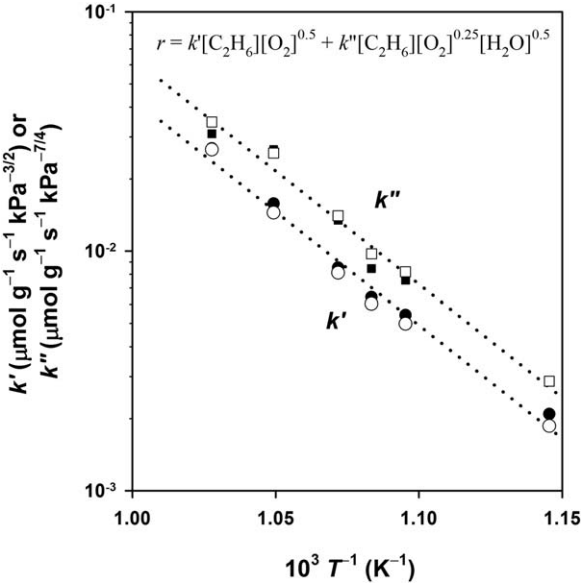

Figure 4. Arrhenius plot for k′ (sphere) and k″ (square) in the equation (Na_2WO_4/SiO_2 0.8 g, C_2H_6 10 kPa, O_2 1.7 kPa (open symbol) or 3.3 kPa (solid symbol), H_2O 0 or 3.2 kPa).

activate the C–H bond even in CH_4 below 673 K and generate methyl radicals.[19] For the OH radical pathway, the enthalpy ΔH_{OH} of the quasi-equilibrated steps of OH radical formation (reaction 4) is 650 kJ mol^{-1}.[21] The reported activation energy $E_{a,OH}$ for the H-abstraction by OH radical from C_2H_6 (reaction 5) at 923 K is ~4 kJ mol^{-1}.[22]

$$E''_{a,app} = E_{a,OH} + \frac{1}{4}\Delta H_{OH} \tag{11}$$

The expected apparent activation energy is ~167 kJ mol^{-1}, which is close to the measured value of 181 kJ mol^{-1}.

The attainable yield in a single-pass reactor was investigated by increasing the temperature to 1073 K as a set temperature, and H_2O was co-fed into the C_2H_6/O_2 mixture. Here, we did not attempt to isolate the surface kinetic pathways or avoid exotherms from the reaction; instead, we attempted to achieve high conversions in a single pass with concurrent homogeneous gas-phase pathways. Figures 5A, B show the C_2H_4 selectivity and yield, respectively, as a function of C_2H_6 conversion. The reaction conditions were 1073 K, 5–20 kPa C_2H_6, 2.3 kPa H_2O, and C_2H_6/O_2 = 1–6, and four different space velocities were set to vary the conversion. High C_2H_4 selectivity ~90% was achieved up to nearly 50% C_2H_6 conversion. Further increase in conversion reduced the C_2H_4 selectivity obviously because of the secondary reaction of C_2H_4, which is combusted to form CO and CO_2 (where CO selectivity > CO_2 selectivity in the investigated conditions). Under the investigated conditions, the highest C_2H_4 yield of ~61% was experimentally achieved at the C_2H_6 conversion of 82%, whose yield value is among the highest for single-pass conversions.[6] The trend lines of the selectivity and yield in Figures 5A, B are based on the pseudo-first-order rate constants of the scheme, which is described in the figures, where the ratios of rate constants are $k_2/k_1 = 0.28$ and $k_3/k_1 = 0.02$.

$$S_{C_2H_4} = \frac{(1-X)-(1-X)^{\frac{k_2/k_1}{1+k_3/k_1}}}{(\frac{k_2}{k_1}-1-\frac{k_3}{k_1})X} \tag{12}$$

$$Y_{C_2H_4} = \frac{(1-X)-(1-X)^{\frac{k_2/k_1}{1+k_3/k_1}}}{(\frac{k_2}{k_1}-1-\frac{k_3}{k_1})} \tag{13}$$

where X, $S_{C_2H_4}$, and $Y_{C_2H_4}$ are the C_2H_6 conversion, C_2H_4 selectivity, and C_2H_4 yield, respectively. The high selectivity at zero conversion suggests that the direct combustion of C_2H_6 is minimal, which is consistent with the low value of $k_3/k_1 = 0.02$. The results under different conditions follow a single trend line, which suggests that the C_2H_4 selectivity is not largely affected by the C_2H_6 and O_2 pressures. The insensitivity of the selectivity to the C_2H_6 pressure suggests that the pseudo-first-order assumption is valid; i.e., the main pathway goes through the dehydrogenation of ethane to ethylene and the subsequent combustion of C_2H_4. Moreover, there is no change in C_2H_4 selectivity at different O_2 pressures among the given conversion levels, which suggests that the kinetic order for oxygen is similar for both the C_2H_6 and C_2H_4 reactions.

$$C_2H_4 + * \overset{K_{C_2H_4}}{\rightleftharpoons} C_2H_{4(s)} \tag{14}$$

$$C_2H_{4(s)} + O_{(s)} \xrightarrow{k_{O,C_2H_4}} C_2H_3\cdot + OH_{(s)} (+*) \tag{15}$$

$$C_2H_4 + OH\cdot \xrightarrow{k_{OH,C_2H_4}} C_2H_3\cdot + H_2O \tag{16}$$

Reactions 15 and 16 show that the C_2H_4 conversions use identical oxidants ($O_{(s)}$ or OH·) to the C_2H_6 conversions

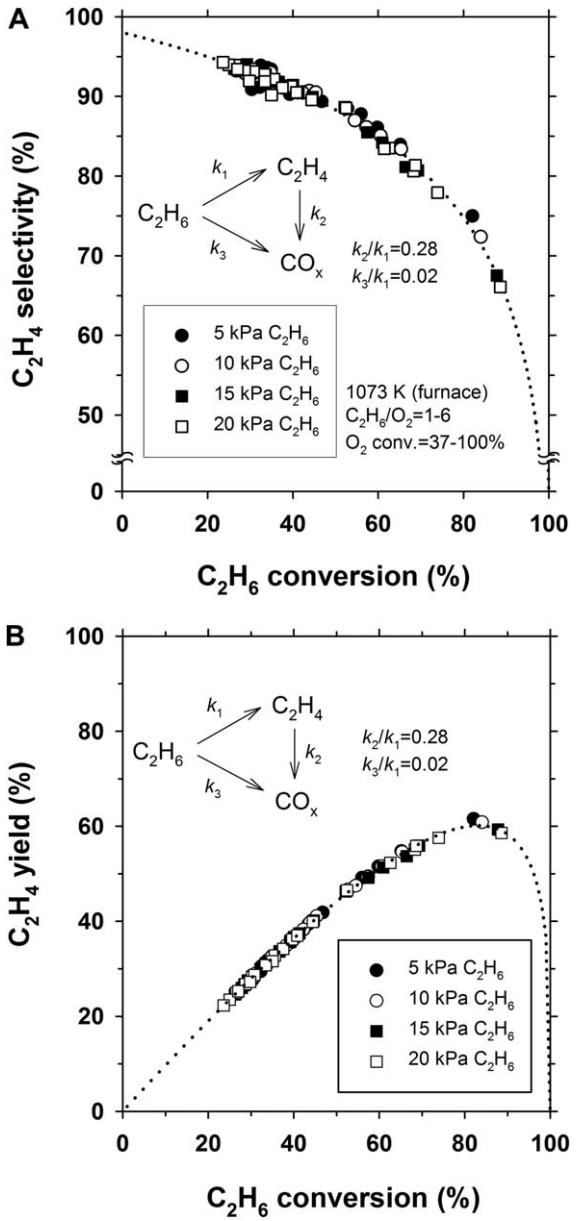

Figure 5. (A) C_2H_4 selectivity and (B) C_2H_4 yield as a function of the C_2H_6 conversion at various partial pressures and residence time (1073 K, Na_2WO_4/SiO_2 0.8 g, C_2H_6 5–20 kPa, $C_2H_6/O_2 = 1$, 3, 5, and 6, H_2O 2.3 kPa, residence time 0.27–0.8 g s cm^{-3}).

(reactions 3 and 5). Thus, we consider that the oxygen membrane does not help improve the C_2H_4 selectivity but may benefit by controlling the reaction rate and resultant exotherms. It is worth noting that in the previous study, a high H_2O/O_2 ratio made the O_2 chemisorption step kinetically relevant for OCM.[16] This argument should be applicable for ODH; however, the oxidant to activate the C–H bond in C_2H_6 and C_2H_4 is similar in this kinetic regime, which should not drastically perturb the selectivity.

The overall attainable yield was determined based on the ratio of rate constants k_2/k_1 in the pseudo-first-order scheme in Figures 5A, B. Because k_3/k_1 is negligibly small, we simplified k_2/k_1 to be the ratio of the overall conversion rate constants of C_2H_6 and C_2H_4 ($k_{C_2H_4}/k_{C_2H_6}$), i.e., the relative C–H bond activation for C_2H_6 vs. C_2H_4. The adsorption of hydrocarbons on the surface may affect the rate if the surface reaction pathway with adsorbed hydrocarbon species is involved in the reaction (compare reactions 2 and 14). C_2H_4 is expected to have a larger adsorption coefficient than C_2H_6 because C_2H_4 contains π-electrons ($K_{C_2H_4} > K_{C_2H_6}$, although experimental values are not available for the relevant catalyst surface). This difference accounts for the rapid combustion on the surface of C_2H_4 relative to C_2H_6, particularly when there is an acid site on the surface. The OH radical pathway in the gas phase is essentially beneficial to improve the C_2H_4 yield if the preferential adsorption of C_2H_4 as an unsaturated hydrocarbon is avoided. In homogeneous gas phase reactions, the rate constants of C_2H_6 and C_2H_4 activation are reported with various H-abstractors. Table 1 shows the rate constants and their ratios of representative reactants (O_2, OH·, O·, H·) to activate the C–H bond from C_2H_6 and C_2H_4 at 923 and 1073 K.[22] In all cases, C_2H_6 reacts more rapidly than C_2H_4, which apparently reflects the weaker C–H bond energy (C_2H_6: 423 kJ mol^{-1}, C_2H_4: 463 kJ mol^{-1}).[20] Generally, a weaker H-abstracter gives a higher $k_{C_2H_4}/k_{C_2H_6}$ ratio.[15] The OH radical is one of the strongest H-abstractors, so it has a relatively high $k_{C_2H_4}/k_{C_2H_6}$ ratio of 0.37, which is not drastically perturbed with the change in reaction temperature (Table 1). The measured $k_{C_2H_4}/k_{C_2H_6}$ ratio of 0.28 during the ODH is close to this value, but the lower value certainly implies that the weaker H-abstractor is likely involved, which slightly reduces $k_{C_2H_4}/k_{C_2H_6}$. It is re-emphasized that the selective catalyst for the ODH of C_2H_6 to C_2H_4 should make less reactive O species without inducing a preferential adsorption of unsaturated hydrocarbon (C_2H_4) over saturated hydrocarbon (C_2H_6).

This study demonstrates detailed kinetic analyses and provides accurate description of the attainable product yield for a relatively high-temperature ODH of ethane reaction that involves radical chemistry. The unique characteristic of the Na-based catalyst (Na_2WO_4/SiO_2) is the large increase in C_2H_6 rates because of water, whose kinetics is consistent with the quasi-equilibrated formation of OH radicals and subsequent C–H bond activation of C_2H_6. Our careful kinetic analyses in this study suggest new insights to unite some discrepancies in the literature of the active sites and mechanistic aspects.

Table 1. Rate Constants and Their Ratio of C–H Bond Activation Using Various H-Abstractors for C_2H_6 and C_2H_4 at 923 and 1073 K[22]

H-abstractor	Hydrocarbon	k at 923 K	$k_{C_2H_4}/k_{C_2H_6}$	k at 1073 K	$k_{C_2H_4}/k_{C_2H_4}$
O_2	C_2H_6	1.37×10^{11}	0.20	3.53×10^{11}	0.24
	C_2H_4	2.72×10^{10}		8.30×10^{10}	
OH	C_2H_6	6.11×10^{12}	0.36	8.54×10^{12}	0.37
	C_2H_4	2.21×10^{12}		3.13×10^{12}	
O	C_2H_6	2.11×10^{13}	0.15	3.13×10^{13}	0.14
	C_2H_4	3.24×10^{12}		4.29×10^{12}	
H	C_2H_6	1.86×10^{13}	0.46	2.83×10^{13}	0.55
	C_2H_4	8.54×10^{12}		1.56×10^{13}	

Conclusions

Our rigorous kinetic analyses for the ODH of C_2H_6 using the Na_2WO_4/SiO_2 catalyst unveil a predominant reaction pathway and a quantitative, mechanism-based description of the attainable C_2H_4 yield. The incremental rates for C_2H_6 conversion that are introduced by the presence of H_2O are consistent with the mechanism of quasi-equilibrated OH radical formation and subsequent C–H bond activation of C_2H_6 as a kinetically relevant step. The C_2H_4 selectivity was insensitive to the C_2H_6 and O_2 pressures, which universally describes the attainable yield by ratios of pseudo-first-order rate constants in hydrocarbons. The measured ratio of rate constants (k_{C2H4}/k_{C2H6}) was 0.28; the high C_2H_4 selectivity was ~90% at 50% C_2H_6 conversion, and the maximum C_2H_4 yield was ~61% at the C_2H_6 conversion of 82%. This study demonstrates the unique but consistent kinetic data for selective dehydrogenation reaction using radical reactions that are initiated by the catalyst surfaces. This information is benchmarking for similar hydrocarbon transformations using alkali-metal-based catalysts.

Acknowledgment

The research reported in this publication was supported by funding from King Abdullah University of Science and Technology (KAUST).

Literature Cited

1. Cavani F, Trifiro F. The oxidative dehydrogenation of ethane and propane as an alternative way for the production of light olefins. *Catal Today*. 1995;24:307–313.
2. Kung HH. Oxidative dehydrogenation of light (C_2 to C_4) alkanes. *Adv Catal*. 1994;40:1–38.
3. Mamedov EA, Cortés Corberán V. Oxidative dehydrogenation of lower alkanes on vanadium oxide-based catalysts. The present state of the art and outlooks. *Appl Catal A*. 1995;127:1–40.
4. Cavani F, Trifiro F. Selective oxidation of light alkanes: interaction between the catalyst and the gas phase on different classes of catalytic materials. *Catal Today*. 1999;51:561–580.
5. Cavani F, Ballarini N, Cericola A. Oxidative dehydrogenation of ethane and propane: how far from commercial implementation? *Catal Today*. 2007;127:113–131.
6. Gärtner CA, van Veen AC, Lercher JA. Oxidative dehydrogenation of ethane: common principles and mechanistic aspects. *ChemCatChem*. 2013;5:3196–3217.
7. Morales E, Lunsford JH. Oxidative dehydrogenation of ethane over a lithium-promoted magnesium oxide catalyst. *J Catal*. 1989;118:255–265.
8. Labinger JA, Ott KC. Mechanistic studies on the oxidative coupling of methane. *J Phys Chem*. 1987;91:2682–2684.
9. Campbell KD, Lunsford JH. Contribution of gas-phase radical coupling in the catalytic oxidation of methane. *J Phys Chem*. 1988;92:5792–5796.
10. Labinger JA. Oxidative coupling of methane: an inherent limit to selectivity? *Catal Lett*. 1988;1:371–376.
11. Mims CA, Mauti R, Dean AM, Rose KD. Radical chemistry in methane oxidative coupling: tracing of ethylene secondary reactions with computer models and isotopes. *J Phys Chem*. 1994;98:13357–13372.
12. Colussi AJ, Amorebieta VT. Optimum yield of the purely heterogeneous oxidative dimerization of methane. *J Catal*. 1997;169:301–306.
13. Su YS, Ying JY, Green WH. Upper bound on the yield for oxidative coupling of methane. *J Catal*. 2003;218:321–333.
14. Takanabe K. Catalytic conversion of methane: carbon dioxide reforming and oxidative coupling. *J Jpn Petrol Inst*. 2012;55:1–12.
15. Takanabe K, Iglesia E. Rate and selectivity enhancements mediated by OH radicals in the oxidative coupling of methane catalyzed by $Mn/Na_2WO_4/SiO_2$. *Angew Chem Int Ed*. 2008;47:7689–7693.
16. Takanabe K, Iglesia E. Mechanistic aspects and reaction pathways for oxidative coupling of methane on $Mn/Na_2WO_4/SiO_2$ catalysts. *J Phys Chem C*. 2009;113:10131–10145.
17. Liang Y, Li Z, Nourdine M, Shahid S, Takanabe K. Methane coupling reaction in an oxy-steam stream through an OH radical pathway by using supported alkali metal catalysts. *ChemCatChem*. 2014;6:1245–1251.
18. Palermo A, Vazquez JPH, Lambert RM. *New efficient catalysts for the oxidative coupling of methane*. *Catal Lett*. 2000;68:191–196.
19. Otsuka K, Said AA, Jinno K, Komatsu T. Peroxide anions as possible active species in oxidative coupling of methane. *Chem Lett*. 1987;77–80.
20. Blanksby SJ, Ellison GB. Bond dissociation energies of organic molecules. *Acc Chem Res*. 2003;36:255–263.
21. Chase MW. *J Phys Chem Ref Data*. 1998; 1 NIST-JANAF, Thermochemical Tables, 4th ed, Monograph 9.
22. GRI-Mech v.3.0. Smith GP, Golden DM, Frenklach M, Moriarty NW, Eiteneer B, Goldenberg M, Bowman CT, Hanson RK, Song S, Gardiner WC, Lissianski VV, Qin Z. Avaialble from: http://www.me.berkeley.edu/gri_mech/

Manuscript received Apr. 4, 2016, and revision received July 21, 2016.